Limitations Caused by Sampling and Quantization in Position Control of a Single Axis Robot

Csaba Budai, *Budapest University of Technology and Economics*
(**15.09.2013**, László L. Kovács Dr., *HAS-BUTE Research Group on Dynamics of Machines and Vehicles*)

Abstract

This paper presents the theoretical and experimental investigation of the dynamics of a single degree-of-freedom robotic arm subjected to digital position control. The experimental setup consists of an industrial robot axis, a micro-controller based low-level control unit, and a high-level Matlab/Simulink position controller. The stable domain of operation is calculated in the parameter space of the sampling time and the gains of the applied proportional-derivative (PD) controller. The calculated stability charts are verified by experiments, and the paper reports the limitations on system stability caused by the digital effects and the applied control setup.

1. Introduction

Fast and accurate motion/position control is an important objective in various robotic applications. This is typically achieved by using high gain, decentralized controllers that operate at high sampling rates. Often the digital effects, like the temporal and spatial discretization (sampling and quantization) are neglected in the control design, and these systems are treated as continuous-time systems. However, in some situations these effects can have a strong influence on the dynamics of the controlled system. For example, sophisticated control algorithms may require considerable computational time, which result in a slower sampling rate. In this case, digital effects can cause an intricate dynamic behavior. Moreover, the non-smooth effects, like quantization, dry friction, backlash may lead to chaotic motions even at high sampling rates [1,2].

The use of high sampling frequencies may be limited by the control hardware in low cost applications, where the sensor readings and the control calculations are implemented on microcontrollers. In this paper we investigate the PD digital position control of a robotic arm controlled by a custom, microcontroller based hardware. A single axis of an industrial robotic arm is controlled by a microcontroller, and Simulink® Real-Time Workshop® [3] is used to provide a flexible user interface for setting the desired positions of the robot. This architecture has the advantage of developing an easy-to-use experimental setup, but it may cause further processing delay and synchronization problems that can lead to instabilities. This is confirmed in the second part of the paper, where an explanation is also provided for the differences observed between the theoretical and practical stability limits.

2. Experimental Setup

The investigated experimental setup consist of a single axis robotic arm (HIRATA MB-H230) controlled by a custom-, self-developed control unit. This low-level controller is based on a PIC microcontroller (24FJ128GA010) that communicates with a Simulink Real-Time Workshop (RTW) based high-level controller by using RS-232 protocol. The microcontroller based platform processes the measured data from the motor encoders, and transmits the calculated angle to the PC. The RTW based control software determines the necessary control force, and transmits it via the microcontroller based platform to the H-bridge in the form of a pulse-width-modulation (PWM) signal. The schematic of the experimental setup can be seen in Fig.1. Here, the single axis industrial robotic arm is shown as a ball screw which is connected to the shaft of the DC motor by a rigid clutch.

The lead of the ball screw is $l = 20$ mm which gives the travelled distance along the robot axis per motor revolutions.

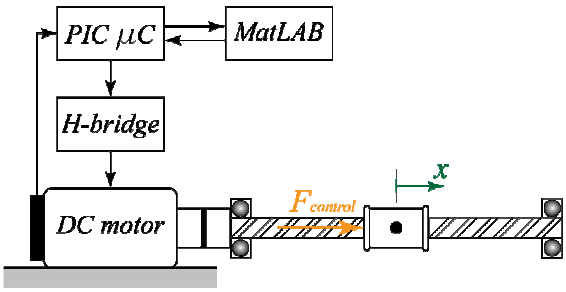

Fig.1. Schematic of the Experimental Setup

Assuming an ideal (lossless) force-torque transmission of the ball screw, the end-effector force is $f = r_t M$, where M is the applied motor torque, and $r_t = 2\pi / l = 100\pi$ is the transmission ratio. The motor torque can be approximated by considering the steady state motor characteristics. Then applying the Biot-Savart's Law [4] the motor torque is $M = k_m i$, where $k_m = 0.1187$ Nm/A is the motor constant and $i = U_m / R$ is the current that flows through the motors windings. Here, $R = 1.1\,\Omega$ is the terminal resistance and U_m is the supply voltage of the motor.

Based on Lenz's Law [4] the motor supply voltage is proportional to its angular velocity. Thus a simple way to control the speed of a DC motor is using a PWM signal to set the average supply voltage. It can be written as $U_m = U_0 p_c / p_m$, where $U_0 = 24$ V is the supply voltage of the H-bridge, p_c is the calculated duty cycle, and $p_m = 730$ is the maximum of the PWM duty cycle. Note, that the value of p_m is limited by the settings (e.g., selected PWM frequency) of the microcontroller, and the quantization of the control force is inversely proportional to this value.

In voltage control mode, the motor torque calculated so far is reduced by the back electromotive force. According to Faraday's Law of Induction [4], this force (torque) is proportional to the angular velocity of the motor shaft. Therefore, it may be considered as a viscous damping force in modeling the actuated robot axis, while the force component proportional to the modulated supply voltage may be seen as the exogenous control force.

By using the previous derivations, this control force can be determined with respect to the duty cycle of the pulse width modulation signal as

$$F = \frac{r_t k_m U_0}{R p_m} p_c = 0.9845\, p_c . \qquad (1)$$

3. The Equivalent Mechanical Model

By using voltage control, and modeling the back EMF effect as a viscous damping element, the simplified mechanical model of the experimental setup is shown in Fig.2.

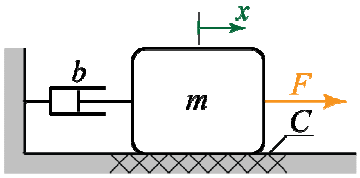

Fig.2. Equivalent Mechanical Model

The equation of motion of this model is

$$m\ddot{x} + b\dot{x} + C\,\mathrm{sgn}(\dot{x}) = F, \qquad (2)$$

where m is the effective mass that represents the robot's inertia, and b is the damping induced by the back EMF effect. Parameter $C \approx 20$ N is the measured Coulomb friction force, while the control force F is defined by eq. (1).

The effective parameters of this model were identified in two simple experiments: (a) accelerating with constant force, and (b) measuring how the system comes to rest due to the viscous damping and dry friction only. By considering a constant positive control force, $\mathrm{sgn}(\dot{x}) = 1$ in eq. (2), then the general solution of the equation of motion becomes

$$x(t) = c_1 + c_2 \mathrm{e}^{-\frac{b}{m}t} + \frac{F - C}{b} t, \qquad (3)$$

where c_1 and c_2 are the constant that depend on the initial conditions. By appropriately selecting the initial position, c_1 can be canceled, while the exponential term vanishes by time. For a constant force input, the steady state solution is

$$x(t) = \frac{F - C}{b} t. \qquad (4)$$

Therefore the effective viscous damping can be calculated as $b = (F - C) / s_b \approx 1443$ Ns/m, where $s_b \equiv v_0 \approx 0.492$ m/s is the slope of the linear segment (the steady state velocity) in Fig.3.

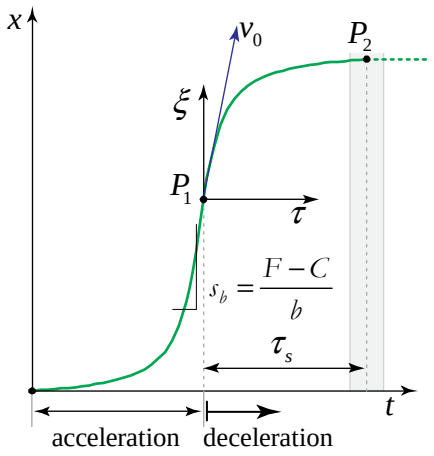

Fig.3. Typical robot motion in parameter identification experiments

The steady state velocity can be seen as the initial velocity of our second experiment with zero control force. The corresponding decelerating motion starts at P_1 in Fig. 3., where also a new coordinate frame is introduced to describe this motion. Point P_2 is the point where the robot stops due to dry friction and viscous damping. The corresponding time $\tau_s \approx 93\,\text{ms}$ was determined as the mean of some uncertain values in the region where the tangent of the curve in Fig 3. becomes zero. Based on eq. (3), in the new (τ,ξ) frame the displacement of the decelerating robot is given by the general solution

$$\xi(\tau) = c_1 + c_2\, \mathrm{e}^{-\frac{b}{m}\tau} - \frac{C}{b}\tau. \qquad (5)$$

Then, with the initial conditions $\xi(\tau=0)=0$ and $\mathrm{d}\xi/\mathrm{d}\tau(\tau=0)=v_0$ the displacement function becomes

$$\xi(\tau) = \frac{m}{b}\left(v_0 + \frac{C}{b}\right)\left(1 - e^{-\frac{b}{m}\tau}\right) - \frac{C}{b}\tau. \qquad (6)$$

By differentiating this expression with respect to τ and considering the stop condition $\mathrm{d}\xi/\mathrm{d}\tau(\tau=\tau_s)=0$, the effective mass of the model in eq. (2) can be estimated as

$$m = \frac{b\tau_s}{\ln\left(1+\frac{bv_0}{C}\right)} \approx 37\,\text{kg}. \qquad (7)$$

4. Controlled Dynamics

For the analysis of the dynamics of the digitally controlled system we neglect, the otherwise stabilizing, dry friction in eq. (2) and we introduce the control force

$$F = -k_p x_{j-1} - k_d \frac{x_{j-1} - x_{j-2}}{\Delta t}, \; t \in [t_j, t_{j+1}), \qquad (8)$$

where k_p and k_d are the control gains, Δt is the sampling time and t_j denotes the j-th sampling instant. In addition, $x_{j-1} = x(t_{j-1})$ and $x_{j-2} = x(t_{j-2})$ represent the sampled and delayed position feedback data [5,6]. The considered single sampling period delay in eq. (8) corresponds to the fact that the Simulink RTW model always transmits the output force first, and processes the received input later in the same control cycle [3].

With these assumptions, the piecewise linear system of equations (2) and (8) can be solved for the consecutive sampling instant, and a linear mapping can be created in the form

$$\mathbf{z}_{j+1} = \mathbf{A}\,\mathbf{z}_j, \qquad (9)$$

where $\mathbf{z}_j = \left[x_j \quad \dot{x}_j\Delta t \quad x_{j-1} \quad x_{j-2}\right]^{\mathrm{T}}$ is the discrete state vector [7,8], and the leading matrix

$$\mathbf{A} = \begin{bmatrix} 1 & \varepsilon & \frac{\varepsilon-1}{\beta}(d+p) & \frac{1-\varepsilon}{\beta}d \\ 0 & 1-\varepsilon\beta & -\varepsilon(d+p) & \varepsilon d \\ 1 & 0 & 0 & 0 \\ 0 & 0 & 1 & 0 \end{bmatrix} \qquad (10)$$

is called the (state) transition matrix. Here, $\varepsilon = (1-\mathrm{e}^{-\beta})/\beta$, and $p = k_p\Delta t^2/m$, $d = k_d\Delta t/m$ and $\beta = b\Delta t/m$ are the dimensionless proportional and differential gains and the dimensionless viscous damping, respectively. To obtain this compact form we defined the elements of the discrete state vector with homogeneous units, i.e., the velocity is scaled by the sampling time. By using eq. (9) with eq. (10) the time series of discrete state values can be determined for any initial condition $\mathbf{z}_0$, and via that the discrete time dynamics of the system can be investigated.

For the proper selection of the control gains the stable domain of operation has to be determined. Since eq. (9) define a multi-dimensional geometric series, by using the trial solution $\mathbf{z}(t) = K e^{\lambda t}$, it can be shown that the system is asymptotically stable if, and only if, the magnitude of largest eigenvalue $\mu = e^{\lambda \Delta t}$, $\mathrm{Re}\{\lambda\} < 0$ of the transition matrix $\mathbf{A}$ is less than one. The corresponding stability conditions can analytically further be analyzed by using the Moebius transformation as shown in [9,10]. For brevity, here we restrict the investigation to the numerical computation of the stable domains.

The system has three control parameters: *p, d* and Δt. With these two practically useful 2D stability charts can be generated. By fixing the sampling time (to its smallest possible value) the stable domain is represented as a D-shaped area in the *p–d* parameter plane.

In voltage control mode, when there is large internal damping due to the back EMF effect, a simple proportional controller is also a valid choice. In this case, the stability chart can be plotted in the $\Delta t - k_p$ plane (with dimensional parameters) instead of using the $\Delta t - p$ plane. These stability charts are illustrated in Fig. 5. and Fig. 6.

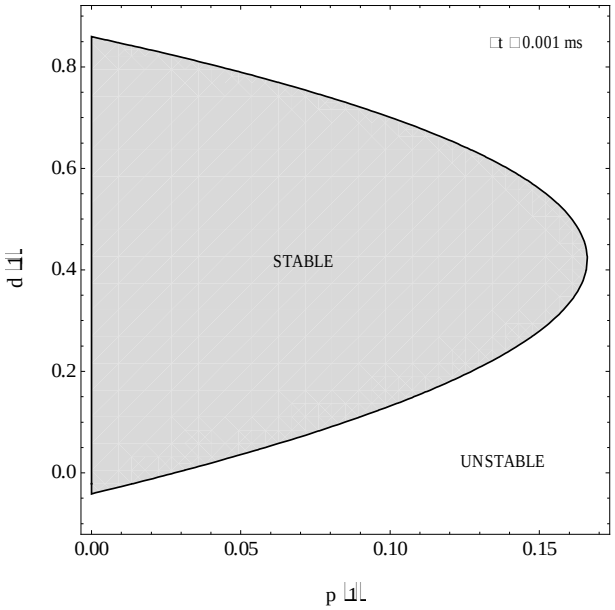

Fig.5. Dimensionless stability chart in p – d plane

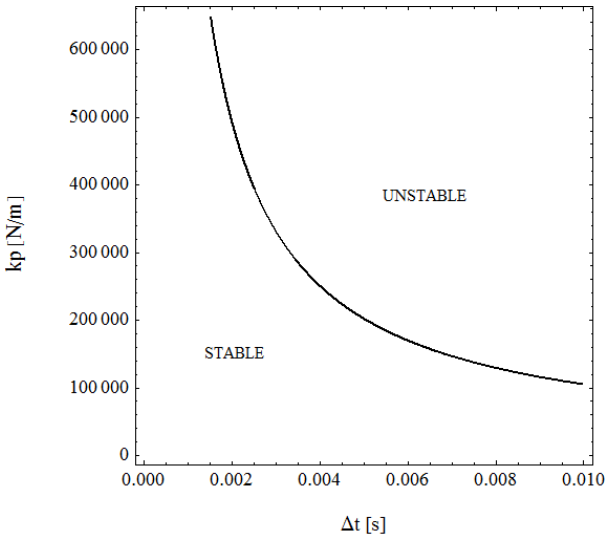

Fig.6. Dimensionless stability chart in Δt – k_p plane

5. Measurement Results

The dynamic analysis presented in the previous section does not consider the effect of the input/output quantization. This effect, however, can have serious effect on the dynamics. Velocity estimation from sampled and quantized position data introduces an error which results in a noisy signal. To eliminate this noise, filtering is necessary which would introduce time delay (phase lag) in the system. In the recent paper, we would like to focus on the possible effects of position quantization only, and we only consider a proportional controller for the experiments. The use of advanced velocity estimators and the effect of quantization noise will be the subject of future investigations.

The theoretical and experimentally identified stability charts are compared in Fig. 7., where Δt is the sampling time, and $P = 0.5 \cdot 10^5 k_p$ is the scaled proportional gain that was used during our experiments. This scaling includes the position quantization and P has the unit of [N/encoder count]. Note, that the resolution of the motor encoder is 1000 cpr which together with the lead $l = 0.02$ m / revolution gives $2 \cdot 10^{-5}$ m/count position resolution for the linear motion of the robot axis.

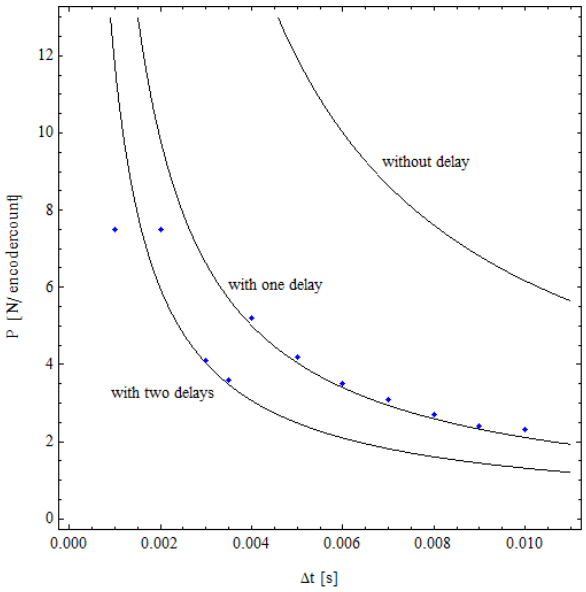

Fig.7. Measured stability chart

The results of our initial experiments are shown in Fig. 7. Here, the theoretical stability boundary is represented by the solid line and the dots show the limits found experimentally at different sampling times. It can be seen that the measured data fit very well to the theoretical boundary in the range of larger (0.01 – 0.004 s) sampling times. For smaller sampling times the system unexpectedly became unstable at lower gains. In addition, it was observed that at $\Delta t = 1\,\text{ms}$ and $\Delta t = 2\,\text{ms}$ the instability occurs exactly at the same gains. These problems could partially be explained by the default settings of the serial communication blocks used in our Simulink RTW model. According to [3], the serial communication block by default has the maximum sampling frequency of 500 Hz. This explains the same dynamic behavior for the experiments with 1 ms and 2 ms sampling times. For smaller sampling times, the RTW documentation [3] suggests the use of the option "direct port access". This option is not documented in detail and the possible improvement is said to be hardware dependent.

Using the direct port access option the experimental results are shown in Fig. 8. From this figure it is apparent that stability was improved in the range $4\,\text{ms} > \Delta t > 2\,\text{ms}$. The points below $\Delta t = 2\,\text{ms}$ seem to fit to a different stability boundary corresponding to the same PD controller with two sampling time delays. This additional delay may be explained by the effect of quantization of the motor encoder. At high sampling rates, the controller may read the same position data repeatedly while the output force remains unchanged. Depending on the measured signal this results in different effective sampling times. The average dynamic behavior may be approximated by a model with two (or more) sampling time delays. This was observed in our experiments, where we used the simplest quadrature (detecting the rising edges only) to process the encoder signals. To increase stability for smaller sampling times the encoder resolution can be improved by quadrature 4X encoding. This is planned as future work.

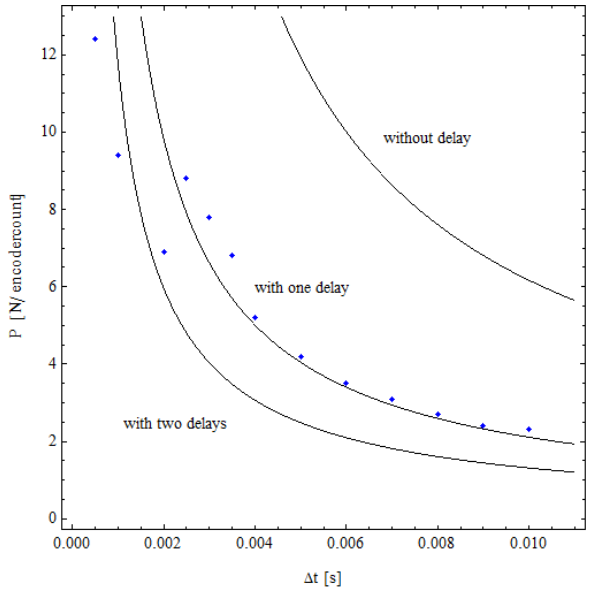

Fig.8. Measured stability chart (with direct port access)

5. Conclusions

In this paper the effect of sampling and quantization was investigated on the system stability in case of a single axis robot subjected to PD digital position control. The theoretical results were compared to experiments conducted on a device with a microcontroller based control unit that interfaces the robot to a high-level Simulink RTW controller.

In case of the investigated experimental setup, the effect of output (force) quantization and dry friction did not have important influence on the system stability. This may be explained by the large viscous damping. On the other hand, it was observed that sampling and input (position) quantization can cause unexpected instability problems even in case of high sampling frequencies.

It is also noted that using a commercial software, like Simulink Real-Time Workshop, the default options, and the applied real-time update mechanism have important effects on system stability which requires careful testing and analysis.

Bibliography

[1] Csernák, G., Stépán, G.: *Sampling and Round-off, as Sources of Chaos in PD-controlled Systems,* Proceedings of The 19th Mediterranean Conference on Control and Automation. Corfu, Greek, 06.20-06.23, pp. 1319-1324, 2011

[2] Csernák, G., Stépán, G.: *Digital control as source of chaotic behavior,* International Journal of Bifurcation and Chaos 20:(5) pp. 1365-1378, 2010

[3] MathWorks: *Simulink Coder (formerly Real-Time Workshop)*, URL: http://www.mathworks.com/products/simulink-coder/, 15.09.13

[4] Petrik O., Huba A., Szász G.: *Rendszertechnika* Budapest, Tankönyvkiadó, 1986 (in Hungarian)

[5] Stépán, G.: *Retarded Dynamical System,* Longman, Harlow, 1989

[6] Insperger T., Stépán G.: *Semi-Discretization for Time-Delay Systems,* Budapest, Springer, 2011

[7] Kovács L.L., Kövecses J., Stépán, G.: *Analysis of effects of differential gain on dynamic stability of digital force control,* International Journal of Non-Linear Mechanics, Elsevier, vol. 43, 514-520, 2008

[8] Insperger, T., Kovács, L.L., Galambos, P., Stépán, G.: *Increasing the accuracy of digital force control process using the act-and-wait concept*, IEEE/ASME Transactions on Mechatronics, 15(2), pp. 291-298, 2010

[9] Magyar, B., Hős Cs., Stépán G.: *Influence of Control Valve Delay and Dead Zone on the Stability of a Simple Hydraulic Positioning System,* Mathematical Problems in Engineering 11: 15 p. Paper 349489, 2010

[10] Stépán, G., Steven, A., Maunder, L.: *Design principles of digitally controlled robots,* Mech. Mach. Theory 25, 515–527, 1990

Authors

MSc Eng Csaba Budai
Dept. of Mechatronics, Optics and Mechanical Engineering Informatics,
Budapest University of Technology and Economics,
H-1521 Budapest, Hungary
tel.: (+36-1) 463-2134

e-mail: *budaicsaba@mogi.bme.hu*

László L. Kovács Dr
HAS-BUTE Research Group on Dynamics of Machines and Vehicles,
H-1521 Budapest, Hungary
tel.: (+36-1) 463-3678

e-mail: *kovacs@mm.bme.hu*